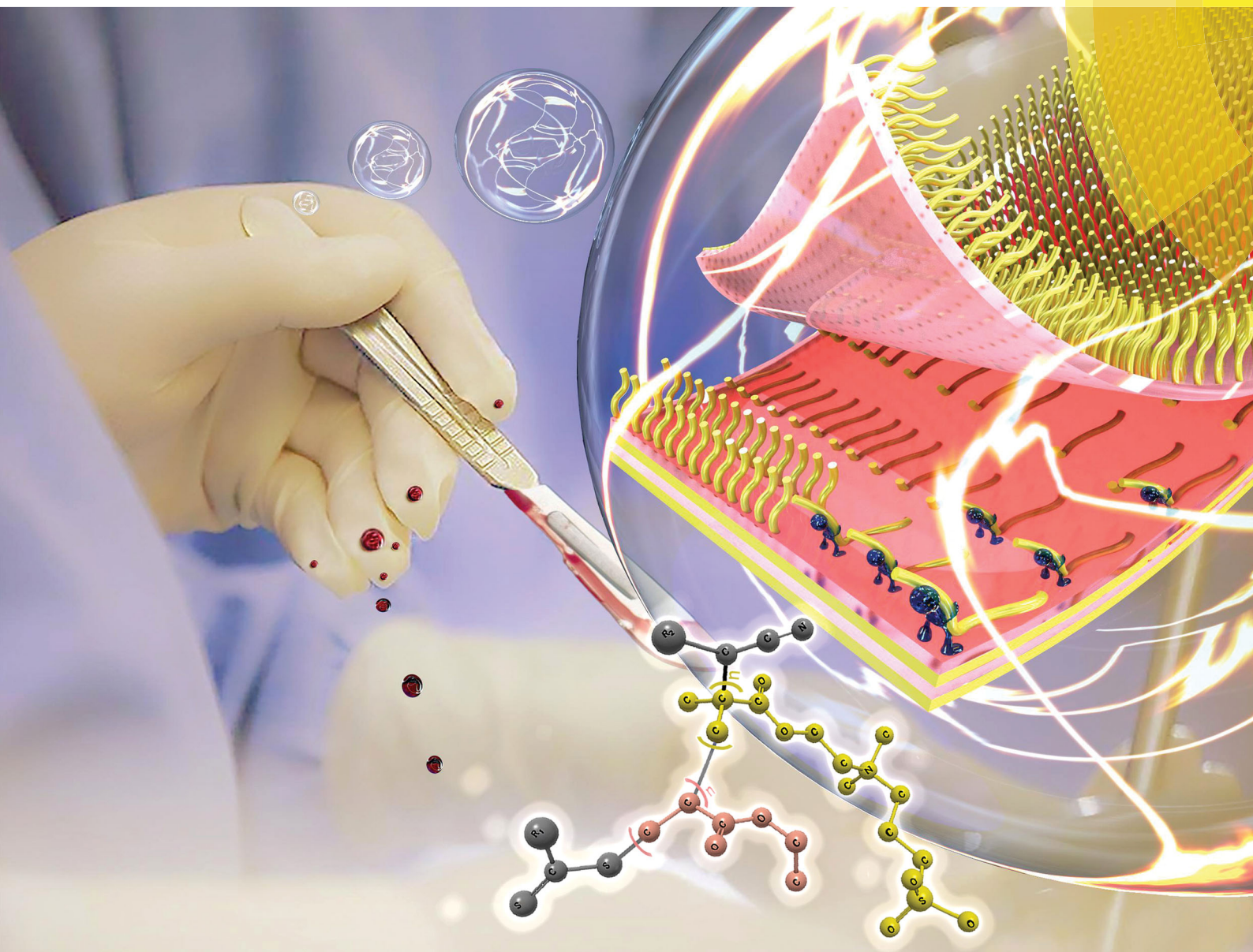


# Journal of Materials Chemistry B

Materials for biology and medicine

[rsc.li/materials-b](http://rsc.li/materials-b)



ISSN 2050-750X



## COMMUNICATION

Han Zuilhof *et al.*

Dual water-healable zwitterionic polymer coatings for anti-biofouling surfaces



## Dual water-healable zwitterionic polymer coatings for anti-biofouling surfaces†

Zhanhua Wang,<sup>ab</sup> Guoxia Fei,<sup>a</sup> Hesheng Xia<sup>ab</sup> and Han Zuilhof<sup>abcd</sup>

Cite this: *J. Mater. Chem. B*, 2018, **6**, 6930

Received 18th July 2018,  
Accepted 14th August 2018

DOI: 10.1039/c8tb01863d

rsc.li/materials-b

Herein, we show for the first time drop-casting zwitterionic polymer colloidal particles onto different surfaces to obtain zwitterionic coatings with highly protein-repelling properties and dual self-healing capabilities. Upon nano/micro mechanical scratches, the coatings self-heal in a NaCl solution which is accompanied by the recovery of the anti-biofouling characteristics. Also under severe macro damage conditions, water will induce the zwitterionic groups buried inside the particles to transfer to the coating surface, and as such regenerate the surface-wetting properties and repair the anti-biofouling properties.

Self-healing polymer materials have drawn great attention in recent years because self-healing can in principle extend the lifetime of materials significantly.<sup>1,2</sup> The first generation of self-repairing polymer materials focuses on the self-healing chemistry and the recovery of structural and mechanical properties<sup>3</sup> based on the dynamic formation of reversible chemical bonding,<sup>4</sup> or irreversible crosslinking.<sup>5–7</sup> Current research interests in self-healing materials are gradually moving from restoring mechanical and structural properties<sup>8</sup> to healing functions, such as conductivity,<sup>9</sup> antifogging,<sup>10</sup> anti-corrosion<sup>11</sup> and anti-fouling properties.<sup>12–15</sup> One of the hottest topics in this field focusses on repairable surface properties, such as wetting and anti-biofouling properties,<sup>16</sup> which can be lost under physical wear or chemical degradation.<sup>17</sup> This is highly relevant to *e.g.* biomedical devices: if the anti-fouling properties of blood-contacting devices with anti-fouling coatings are lost over time, the chance of thrombosis in/around such devices will increase.<sup>18</sup> This limits to some degree,

for mechanically challenging applications, the use of anti-fouling polymer brushes: the initial antifouling properties may be really high,<sup>19–24</sup> but due to the highly restricted mobility of the brushes – which is covalently bonded onto the surface – this coating is very difficult to be repaired.

Several recent studies have therefore focused on retaining or restoring anti-fouling properties after damage by the development of self-healing coatings. There are two main kinds of self-healing anti-fouling systems which focus on the repair of different extents of surface damage: a small scale or a larger scale. The first aims to implement flexibility in the shape of the material, so that in the case of a small scratch material at both sides of the cut can contact again. This is important, as fouling biomolecules will typically be easily trapped into the scratch, and as such generate biofouling; repair of the scratch will also repair the anti-biofouling properties. In this category, Sun's group reported a self-assembly-based coating consisting of PEGylated branched poly(ethylenimine) and hyaluronic acid assembled multilayer films.<sup>25</sup> Our previous work on zwitterionic polymer networks<sup>26</sup> (see below for more discussion) also falls into this category. The second kind refers to macro damage, in which case the actual loss of the material may occur. In this category, more mechanically sturdy materials have been used, which allow surface restructuring upon abrasion-induced damage and removal of surface constituents. In this category, Sergio's group developed 3D cross-linked networks by the grafting of poly(ethylene oxide) onto cross-linked poly(2-vinyl pyridine) (P2VP) films. In the case of macro damage, slicing away of the material at the surface of the layer leads to P2VP being on top, and thus to the reduction of anti-biofouling properties. Replacement of the detached or damaged polymeric chains by the segments of the PEG chains stored inside the film in proximity to the interface can then induce the further regeneration of the surface-functional PEG segments and concomitant repair.<sup>27</sup> In this case the damaged surface cannot fully recover to the original state due to the loss of material, but at least the surface function can be kept intact by regenerating the surface structure and composition. Analogously, assembling

<sup>a</sup> State Key Lab of Polymer Materials Engineering, Polymer Research Institute of Sichuan University, Chengdu, 610065, P. R. China

<sup>b</sup> Laboratory of Organic Chemistry, Wageningen University, Stippeneng 4, 6708 WE, Wageningen, The Netherlands. E-mail: Han.Zuilhof@wur.nl

<sup>c</sup> School of Pharmaceutical Science and Technology, Tianjin University, 92 Weijin Road, Nankai District, Tianjin, P. R. China

<sup>d</sup> Department of Chemical and Materials Engineering, King Abdulaziz University, Jeddah, Saudi Arabia

† Electronic supplementary information (ESI) available: Experiment details, IR spectra, DLS data and microscopy images. See DOI: 10.1039/c8tb01863d

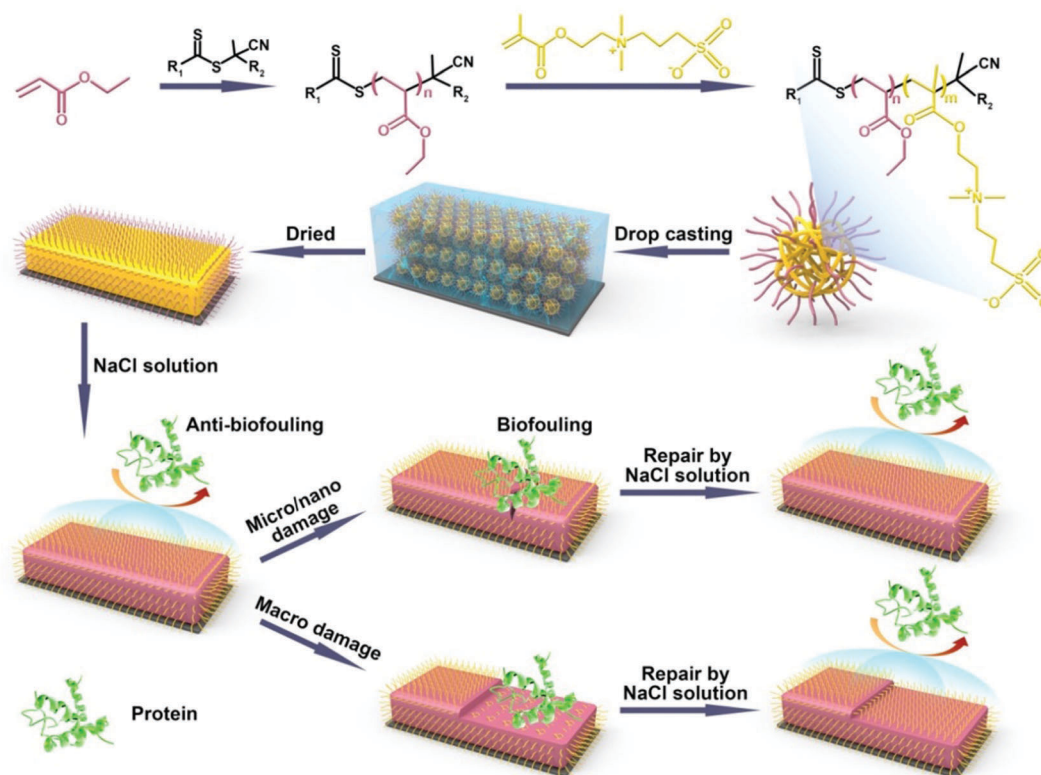


silica-enforced microspheres composed of a hydrophilic core and hydrophobic protecting shells have been advocated as another way to achieve repairable anti-biofouling coatings.<sup>28,29</sup>

In our previous work, we developed a new kind of zwitterionic polymer coating (zwitterionic polymers crosslinked with a fine-tuned fraction of PEG chains) that displayed excellent self-healing and anti-biofouling properties.<sup>26</sup> These coatings can be easily applied onto various substrates by spin-coating/drop-casting. No protein adsorption was observed for the freshly prepared zwitterionic coatings, while strong local protein adhesion was found if the coating was scratched at a micro or nanoscale. There we found that the maximum width and depth that can be repaired are related to the coating thickness, as for large degree damage, the coatings cannot be repaired and the protein adsorption still occurs. Up to now, to the best of our knowledge, there has been no report on anti-biofouling coatings which can repair both the nano/micro scratches and macro damage, and substantially regenerate the anti-biofouling properties after the healing process. This is linked to the balance between flexible enough to allow molecular mobility on the one hand, with sufficient structural strength to withstand substantial abrasion and surface restructuring on the other hand. Since the sort and extent of material damage typically cannot be predicted upon long-term day-to-day use, new kinds of anti-biofouling polymer materials that integrate a self-healing structure, mechanical strength and optimal surface properties are in high demand. In addition, we would like this coating to function

under physiologically relevant conditions, *i.e.* salt-containing aqueous media. In order to further improve the self-healing and anti-biofouling properties of the zwitterionic coatings and overcome all of the issues mentioned above, herein we report on a new kind of dual self-healing anti-biofouling coating, which can repair both macro and nano/micro-scale damage and regenerate the surface wetting and anti-biofouling properties.

We thus aimed our coatings to be formed by drop-casting polyethylacrylate (PEA)-*b*-poly-2-[(methacryloyloxy)ethyl]dimethyl-(3-sulfopropyl)ammonium hydroxide (PMEDSAH) microspheres onto the substrates (see Scheme 1). We expected this material to display self-healing behavior, originating from the reversible electrostatic interaction between positive and negative charges, the high swelling degree of the coatings and the interdiffusion of polyelectrolytes. This set of properties has been utilized by others to prepare ultra-strong self-healing hydrogels<sup>30–32</sup> and healable self-assembling layer-by-layer films.<sup>33</sup> We hypothesized that upon nano/micro mechanical scratches, the broken ionic bond between the protonated ammonium group and sulfonic group can be reformed *via* the involvement of aqueous salt solutions, which thereby repairs the damage. The anti-biofouling properties during this damage-repair process should then also be repaired. In the case of larger scale, abrasion-induced damage, this mechanism will not work as the long distance prevents the broken chains from reform. However, immersing the coatings into a salt solution should then allow surface restructuring *via* the induction of the transfer of buried zwitterionic groups to the



**Scheme 1** Schematic illustration of the monomer structures used to prepare the zwitterionic polymer networks and the protein adhesion behavior on the freshly prepared, damaged and repaired zwitterionic polymer networks.





surface, with the regeneration of the surface-wetting properties and the concomitant recovery of its anti-biofouling properties.

PEA-*b*-PMEDSAH microspheres were fabricated by reversible addition-fragment chain transfer (RAFT) polymerization-induced self-assembly. The macro-RAFT reagent was synthesized by polymerizing an EA monomer with 4,4'-azobis(4-cyanovaleric acid) as the initiator and the 4-cyano-4-(phenylcarbonothioylthio)-pentanoic acid as the chain transfer reagent. 2-Methoxyethanol was selected as the solvent, which played a crucial role in the self-assembly process. First of all, it can dissolve both EA and MEDSAH monomers. Secondly, it is also a good solvent for PEA. Finally, and most importantly, while it can dissolve the MEDSAH monomer, it cannot dissolve PMEDSAH, which induces – during the polymerization of the MEDSAH block to yield the block copolymer PEA-*b*-PMEDSAH – the spontaneous formation of microspheres with a hydrophobic shell and a hydrophilic internal structure (see Scheme 1).<sup>34</sup> PEA was selected because of its hydrophobicity, as it can thus act as a protection layer of the zwitterionic group; PMEDSAH was employed due to its excellent anti-fouling behavior that results from the strong hydration of the zwitterionic moiety.<sup>20,21,35,36</sup> Moreover, the reversible electrostatic interaction between the zwitterionic groups of this zwitterionic polymer network (ZPN) should endow the coatings with excellent self-healing properties.

By tuning the starting ratio between PEA and PMEDSAH, we can obtain the PEA-*b*-PMEDSAH particles with different sizes. When the weight ratio between PEA and PMEDSAH is 3.13, 1.56 and 0.94 – designated as PEA-*b*-PMEDSAH P1, P2 and P3, respectively – we obtain particles with an average size of 78, 115 and 205 nm, respectively, as analyzed by dynamic light scattering (Fig. S1A, ESI†). In order to obtain the ZPN coatings, the PEA-*b*-PMEDSAH microsphere solution was first deposited onto the modified substrates. After evaporating the solvent, the microspheres collapse and adhere to each other, yielding a homogenous coating. The well-dried coating was characterized by FTIR spectra (Fig. S1B, ESI†). The strong peaks at 1730 cm<sup>-1</sup> and 1157 cm<sup>-1</sup> can be attributed to the carbonyl and sulfonyl groups, respectively, and confirm that the PEA-*b*-PMEDSAH copolymer was successfully prepared.

The ability of these coatings to repair small-scale mechanical scratches by simple immersion of damaged films in a NaCl solution was monitored by optical microscopy. Taking the ZPN coating formed by PEA-*b*-PMEDSAH P3 as an example, the bright-field optical images in Fig. 1 show that, after mechanically damaging the coating by scratching the surface more or less vertically with a surgical blade, the scratch disappeared after immersing the surface into 3 wt% NaCl solution for 1 h. This illustrates the ability of ZPN coatings to be repaired by a salt solution. The self-healing process could also be observed by microscopy in real time: the video in the ESI† clearly shows the self-healing process: upon flowing the salt solution over the damaged area, repair of the scratch starts instantly, and finishes in 1 h. In addition, the healing time decreases with the increased ratio between PEA and PMEDSAH. When the ratio is 3.13 and 1.56, respectively, only 5 and 10 min are needed to fully repair the

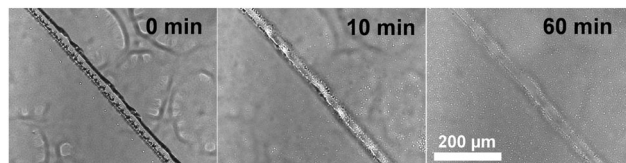


Fig. 1 Optical images of a damaged ZPN coating formed by PEA-*b*-PMEDSAH P3 after being immersed into 3 wt% NaCl for different times.

damage (Fig. S1E–H, ESI†). This is because a higher PEA content make the coating softer, which will accelerate the movement of the polymer chain, further facilitating the healing process. We propose that these self-healing abilities of the coatings originate from the combination of the reversible electrostatic interactions between positive and negative charges, the high swelling degree of the coatings and the interdiffusion of polyelectrolytes at the fractured surfaces in the presence of water. Analogous to our previous work on ZPN coatings,<sup>26</sup> this swelling-based healing mechanism implies that the healing abilities of the coatings are thickness-dependent,<sup>37</sup> because a thicker coating can swell to heal a wider cut.

Due to the self-assembly process, we hypothesized that the outside of the obtained microspheres consisted of PEA chains. This was indeed confirmed by XPS and contact angle measurements. The contact angle of freshly prepared coatings from PEA-*b*-PMEDSAH P3 was  $87 \pm 3^\circ$  (Fig. 2A1), and only carbon and oxygen signals can be observed from the XPS results; specifically, no nitrogen signal was found (Fig. 2A2). These results indicate that there are no PMEDSAH chains on the coating surface, *i.e.* not in the outermost 10–20 nm, given the penetration depth of XPS measurements. After immersion of these coatings into 3 wt% NaCl for 2 days, the microsphere structure of the outermost microspheres was broken, as the PMEDSAH block gradually moves to the top of coatings due to the strong interaction of the PMEDSAH segments with water. This would induce an increase of the surface hydrophilicity, and the static water contact angle indeed decreases to  $28 \pm 2^\circ$  as required to form a functional, antifouling coating. This regeneration process is also related to the ratio between PEA and PMEDSAH. As shown in Fig. S1C (ESI†), the contact angle changes from 104 and 100 to 95 and 67 when the ratio is 3.13 and 1.56 due to the decreased content of the zwitterionic groups in PMEDSAH compared to P3. As reported in the literature, hydrophilic zwitterionic coatings will possess excellent anti-biofouling properties. Therefore, we only use sample PEA-*b*-PMEDSAH P3 to investigate the anti-biofouling properties in the next part. Finally, from Fig. S1C (ESI†), we can also see that the contact angle does not change any more after two days, which means that the surface wetting properties of the coating have reached equilibrium. This further indicates that the as-prepared coatings are stable at least for 7 days in 3 wt% NaCl. More detailed stability tests under standard conditions<sup>38</sup> are under current investigations.

In order to check the anti-biofouling properties of the original, undamaged ZPN coatings, we first immersed the as-prepared (hydrophobic) coatings in a 3 wt% NaCl solution



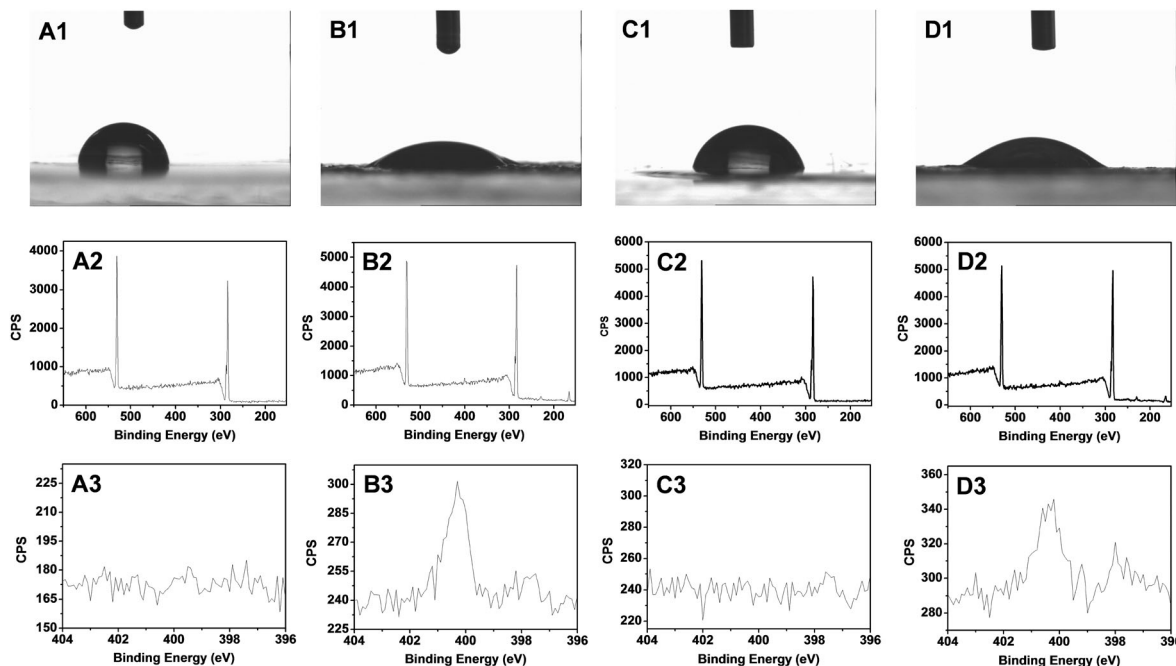


Fig. 2 Characterization of PEA-*b*-PMEDSAH coated surfaces by the static water contact angle (1), XPS wide scan (2) and N1s narrow scan (3) of: (A1–A3) the original PEA-*b*-PSBDSH coatings; (B1–B3) the original PEA-*b*-PMEDSAH coatings after immersion into a 3.0 wt% NaCl solution for 2 days; (C1–C3) the regenerated PEA-*b*-PMEDSAH coatings after damage by a horizontally cutting surgical blade; (D1–D3) the thus damaged PEA-*b*-PMEDSAH coatings after subsequent immersion into a 3.0 wt% NaCl solution for 2 days.

for a specified time (up to 2 days), and then ZPN coatings were covered by a drop of  $0.1 \text{ mg mL}^{-1}$  Alexa Fluor 488-labeled BSA solution for 10 min, and then rinsed ( $5\times$ ) with 2 mL of 10 mM PBS solution and subsequently dried by blowing with argon. Then, the coatings were analyzed by fluorescence microscopy. The protein absorption amount decreases with the increased immersion time (see the ESI,† Fig. S2; this feature is also relevant to the discussion of the repair of macro-damage; see discussion on Fig. 3A3/4 and B3/4, below). After 40 h immersion, the absorbed amount was reduced by a factor of 10. We rationalize this by transfer of an increasing fraction of zwitterionic groups to the top of the surface upon prolonged immersion, which will increase the surface hydration and further reduce protein adsorption.

Next, we examined the effects of damage and self-repair for both micro-damage and macro-damage. The repair of the anti-biofouling properties of microscale-damaged ZPN coatings was investigated upon exposure of the as-obtained, damaged and repaired surfaces to an Alexa 488-BSA solution for 10 min, subsequent washing and local analysis using normal and fluorescence microscopy. When a surface is damaged with a thin cut ( $<10 \text{ }\mu\text{m}$ ; Fig. 3A1), neither the surface nor the cut displays intrinsic fluorescence (Fig. 3A2). When this damaged surface is then placed in a fluorescent protein solution, the protein adsorbs onto the damaged area, as revealed by a locally intense green fluorescence (see *e.g.* Fig. 3B2). In fact, even just contact with such an aqueous solution starts to repair the scratch, as visible in Fig. 3B1: the cut is already thinner than that after the start.

When this experiment is repeated, with a difference that the surface is only placed in the protein solution after first being

repaired in salt water (60 min), then no protein adsorption can be observed in the initially damaged area (Fig. 3D2), even though the optical image (D1) still shows some signs of where the original cut was made. In other words, the repair does not only heal the structure, but also recovers the antifouling properties.

The same method was also employed to examine the anti-biofouling properties of macroscale-damaged and repaired coatings. To obtain reference points that highlight the repair process, first freshly prepared coatings were obtained by drop-casting the PEA-*b*-PMEDSAH solution onto the substrate followed by the evaporation of the solvent. The resulting surface thus displays PEA chains, and is thus somewhat hydrophobic. When this coating (optical image, Fig. 3A3) was immersed into the Alexa 488-BSA solution for 10 min, obvious protein adsorption was found as expected (Fig. 3A4). This amount of adsorbed protein was strongly reduced if the coatings were first regenerated in 3 wt% NaCl for 2 days prior to dipping into the protein solution (see Fig. 3B4). This is interpreted to be due to the surface rearrangement from zwitterionic groups transferring to the coating surface, as referred to before. Next, we purposely damaged the coating over an extended area, by removing (“shaving off”) the top layer with a blade (Fig. 3C3). As a result strong protein adsorption was observed again (Fig. 3C4): we effectively removed part of the surface that displayed zwitterionic moieties, and now again have microspheres on top of the layer that display PEA chains at the outside. As a result, the coating lost the anti-biofouling properties. However, repairing these macro-damaged coatings by immersing them into 3 wt% NaCl for 2 days leads to full repair of the anti-biofouling



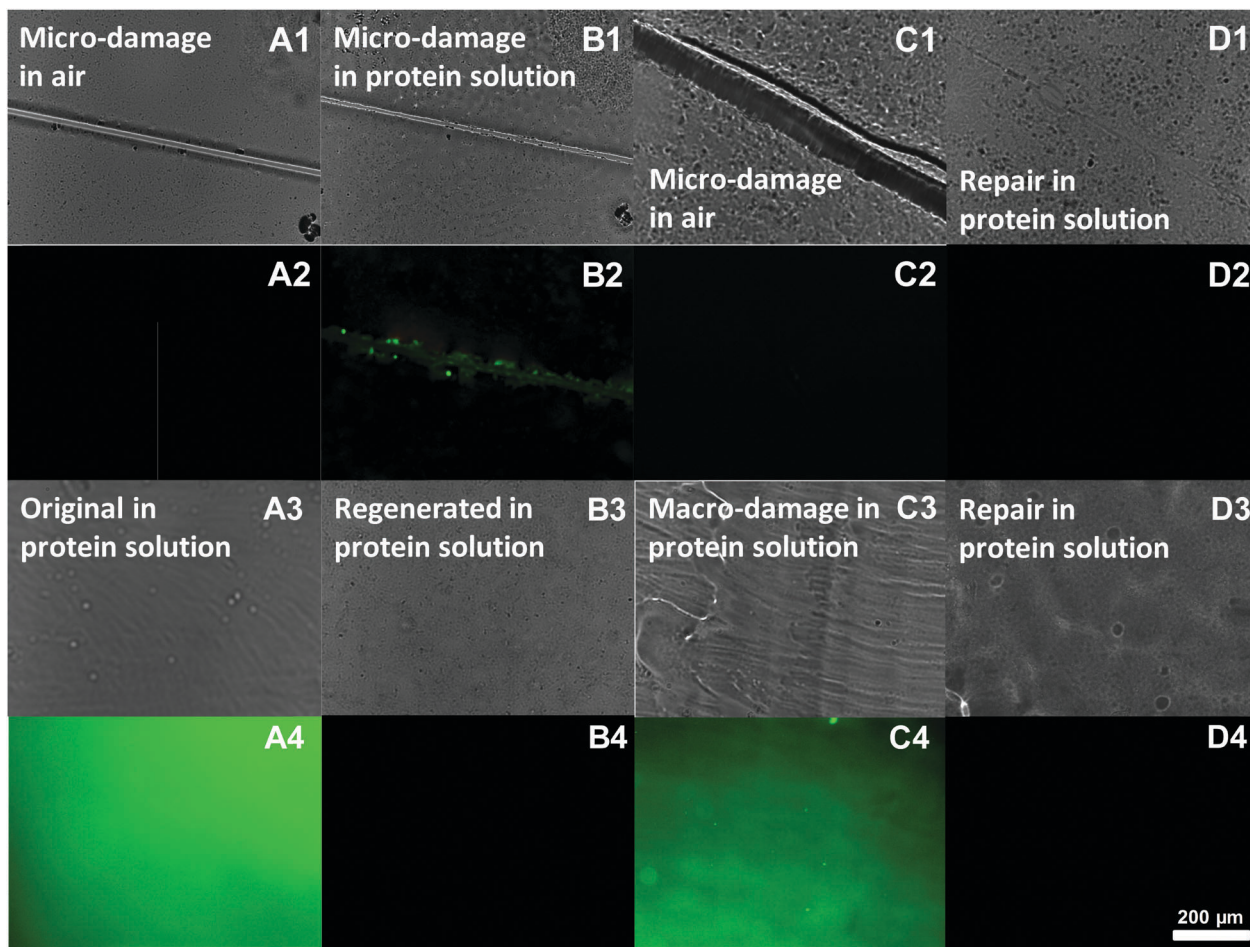


**Fig. 3** Optical (A1 and B1) and fluorescence (A2 and B2) images of the microscale damaged ZPN coatings before (A1 and A2) and after (B1 and B2) immersion into Alexa 488-BSA solution for 10 min. Optical (C1 and D1) and fluorescence (C2 and D2) images of the microscale damaged (C1 and C2) and repaired (D1 and D2) ZPN coatings after immersion into Alexa 488-BSA solution for 10 min. Optical images and fluorescence images of the freshly prepared (A3 and A4), regenerated (immersed into 3 wt% NaCl for 2 days, B3 and B4), macro damaged (C3 and C4) and repaired (D3 and D4) ZPN coatings after immersed into Alexa 488-BSA solution for 10 min. [Note: all images have an equal size and scale bar.]

properties, as afterwards no protein adsorption was observed (Fig. 3D4). This repeatable process thus repairs large-scale damage.

In conclusion, we developed a novel kind of zwitterionic polymer coating by drop-casting PEA-*b*-PMEDSAH core-shell microspheres (hydrophobic outside, hydrophilic inside). Upon immersion into physiologically relevant salt solutions this coating displays a low water contact angle and excellent anti-biofouling properties. Most interestingly, both wetting and anti-fouling properties are fully repaired after both nano/micro scratches and after abrasion-induced macroscale damage *via* the regeneration of the surface chemical composition through simple immersion into a salt solution. These stable, easily prepared, repairable and protein-repellent materials display significant potential applications for long-term stable biosensors and anti-biofouling coatings.

## Conflicts of interest

There are no conflicts to declare.

## Acknowledgements

This project was financially supported by the National Science Foundation of China (NSFC) under Grant No. 51703143 and the State Key Laboratory of Polymer Materials Engineering (Grant No. sklpme2017-3-04).

## Notes and references

- 1 Y. Yang and M. W. Urban, *Chem. Soc. Rev.*, 2013, **42**, 7446–7467.
- 2 J. F. Patrick, M. J. Robb, N. R. Sottos, J. S. Moore and S. R. White, *Nature*, 2016, **540**, 363–370.
- 3 Y. Yang, X. C. Ding and M. W. Urban, *Prog. Polym. Sci.*, 2015, **49–50**, 34–59.
- 4 N. Kuhl, S. Bode, M. D. Hager and U. S. Schubert, in *Self-Healing Materials*, ed. M. D. Hager, S. VanDerZwaag and U. S. Schubert, Springer-Verlag Berlin, Berlin, 2016, vol. 273, pp. 1–58.
- 5 C. E. Diesendruck, N. R. Sottos, J. S. Moore and S. R. White, *Angew. Chem., Int. Ed.*, 2015, **54**, 10428–10447.





- 6 B. Ghosh and M. W. Urban, *Science*, 2009, **323**, 1458–1460.
- 7 Y. Yang and M. W. Urban, *Angew. Chem., Int. Ed.*, 2014, **53**, 12142–12147.
- 8 S. R. White, J. S. Moore, N. R. Sottos, B. P. Krull, W. A. S. Cruz and R. C. R. Gergely, *Science*, 2014, **344**, 620–623.
- 9 Y. Li, S. S. Chen, M. C. Wu and J. Q. Sun, *Adv. Mater.*, 2012, **24**, 4578–4582.
- 10 Y. Wang, T. Q. Li, S. H. Li and J. Q. Sun, *Chem. Mater.*, 2015, **27**, 8058–8065.
- 11 D. V. Andreeva, D. Fix, H. Mohwald and D. G. Shchukin, *Adv. Mater.*, 2008, **20**, 2789–2794.
- 12 Z. H. Wang and H. Zuillhof, *Langmuir*, 2016, **32**, 6310–6318.
- 13 Z. H. Wang and H. Zuillhof, *J. Mater. Chem. A*, 2016, **4**, 2408–2412.
- 14 T. S. Wong, S. H. Kang, S. K. Y. Tang, E. J. Smythe, B. D. Hatton, A. Grinthal and J. Aizenberg, *Nature*, 2011, **477**, 443–447.
- 15 L. Li, B. Yan, J. Q. Yang, L. Y. Chen and H. B. Zeng, *Adv. Mater.*, 2015, **27**, 1294–1299.
- 16 K. L. Chen, Y. Wu, S. X. Zhou and L. M. Wu, *Macromol. Rapid Commun.*, 2016, **37**, 463–485.
- 17 P. C. Zhang, L. Lin, D. M. Zang, X. L. Guo and M. J. Liu, *Small*, 2017, **13**, 1503334.
- 18 B. D. Ippel and P. Y. W. Dankers, *Adv. Healthcare Mater.*, 2018, **7**, 1700505.
- 19 E. van Andel, I. de Bus, E. J. Tijhaar, M. M. J. Smulders, H. F. J. Savelkoul and H. Zuillhof, *ACS Appl. Mater. Interfaces*, 2017, **9**, 38211–38221.
- 20 A. T. Nguyen, J. Baggerman, J. M. J. Paulusse, C. J. M. van Rijn and H. Zuillhof, *Langmuir*, 2011, **27**, 2587–2594.
- 21 Z. Zhang, T. Chao, S. F. Chen and S. Y. Jiang, *Langmuir*, 2006, **22**, 10072–10077.
- 22 Y. C. Hu, B. Liang, L. Fang, G. L. Ma, G. Yang, Q. Zhu, S. F. Chen and X. S. Ye, *Langmuir*, 2016, **32**, 11763–11770.
- 23 S. F. Chen and S. Y. Jiang, *Adv. Mater.*, 2008, **20**, 335–338.
- 24 Y. Higaki, M. Kobayashi, D. Murakami and A. Takahara, *Polym. J.*, 2016, **48**, 325–331.
- 25 D. D. Chen, M. D. Wu, B. C. Li, K. F. Ren, Z. K. Cheng, J. Ji, Y. Li and J. Q. Sun, *Adv. Mater.*, 2015, **27**, 5882–5888.
- 26 Z. H. Wang, E. van Andel, S. P. Pujari, H. H. Feng, J. A. Dijkstra, M. M. J. Smulders and H. Zuillhof, *J. Mater. Chem. B*, 2017, **5**, 6728–6733.
- 27 H. Kuroki, I. Tokarev, D. Nykypanchuk, E. Zhulina and S. Minko, *Adv. Funct. Mater.*, 2013, **23**, 4593–4600.
- 28 W. S. Wang, R. A. Siegel and C. Wang, *ACS Biomater. Sci. Eng.*, 2016, **2**, 180–187.
- 29 K. L. Chen, S. X. Zhou and L. M. Wu, *ACS Nano*, 2016, **10**, 1386–1394.
- 30 F. Luo, T. L. Sun, T. Nakajima, T. Kurokawa, A. Bin Ihsan, X. Li, H. Guo and J. P. Gong, *ACS Macro Lett.*, 2015, **4**, 961–964.
- 31 T. Bai, S. Liu, F. Sun, A. Sinclair, L. Zhang, Q. Shao and S. Jiang, *Biomaterials*, 2014, **35**, 3926–3933.
- 32 F. Luo, T. L. Sun, T. Nakajima, T. Kurokawa, Y. Zhao, K. Sato, A. Bin Ihsan, X. Li, H. Guo and J. P. Gong, *Adv. Mater.*, 2015, **27**, 2722–2727.
- 33 X. Wang, F. Liu, X. W. Zheng and J. Q. Sun, *Angew. Chem., Int. Ed.*, 2011, **50**, 11378–11381.
- 34 M. J. Derry, L. A. Fielding and S. P. Armes, *Prog. Polym. Sci.*, 2016, **52**, 1–18.
- 35 S. Y. Jiang and Z. Q. Cao, *Adv. Mater.*, 2010, **22**, 920–932.
- 36 Q. Shao and S. Y. Jiang, *Adv. Mater.*, 2015, **27**, 15–26.
- 37 J. A. Yoon, J. Kamada, K. Koynov, J. Mohin, R. Nicolay, Y. Z. Zhang, A. C. Balazs, T. Kowalewski and K. Matyjaszewski, *Macromolecules*, 2012, **45**, 142–149.
- 38 N. S. Bhairamadg, S. P. Pujari, F. G. Trovela, A. Debrassi, A. A. Khamis, J. M. Alonso, A. A. Al Zahrani, T. Wennekes, H. A. Al-Turaif, C. Rijn, Y. A. Alhamed and H. Zuillhof, *Langmuir*, 2014, **30**, 5829–5839.

